Expanded View Figure legends

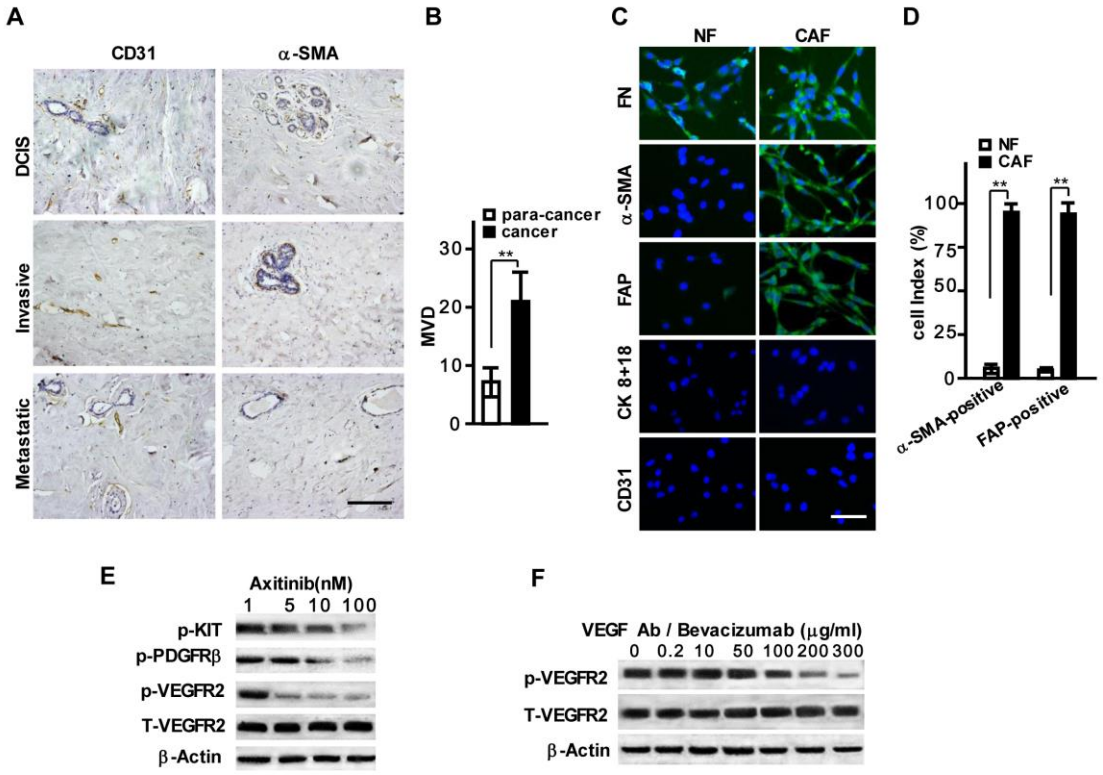

Figure S1. Identification of breast NFs and CAFs and the appropriate concentration of Axitinib and anti-VEGF antibody. (A) Expressions of CD31 and α-SMA in para-cancer (non-tumor) tissues. Scale bar, 200 μm. (B) Quantity of MVD in para-cancer and cancer tissues. (C) Identification of NFs and CAFs which are positive for FN, negative for CK8+18 and CD31; Scale bar, 100 μm. (D) α-SMA and FAP positive cell counts were evaluated under a fluorescence microscope, more than 95% of CAFs were positive for α-SMA and FAP. (E) Western blotting analysis was used to detect total and phosphorylated VEGFR2, phosphorylated KIT and PDGFRβ proteins in HUVECs treated with different concentration of VEGFR2 inhibitor axitinib for 6 hours. (F) Western blotting analysis was used to detect total and phosphorylated VEGFR2 proteins in HUVECs incubated in CM from CAF neutralized with a different concentration of anti-VEGF antibody (bevacizumab). β-Actin is the loading control. (**P<0.01).

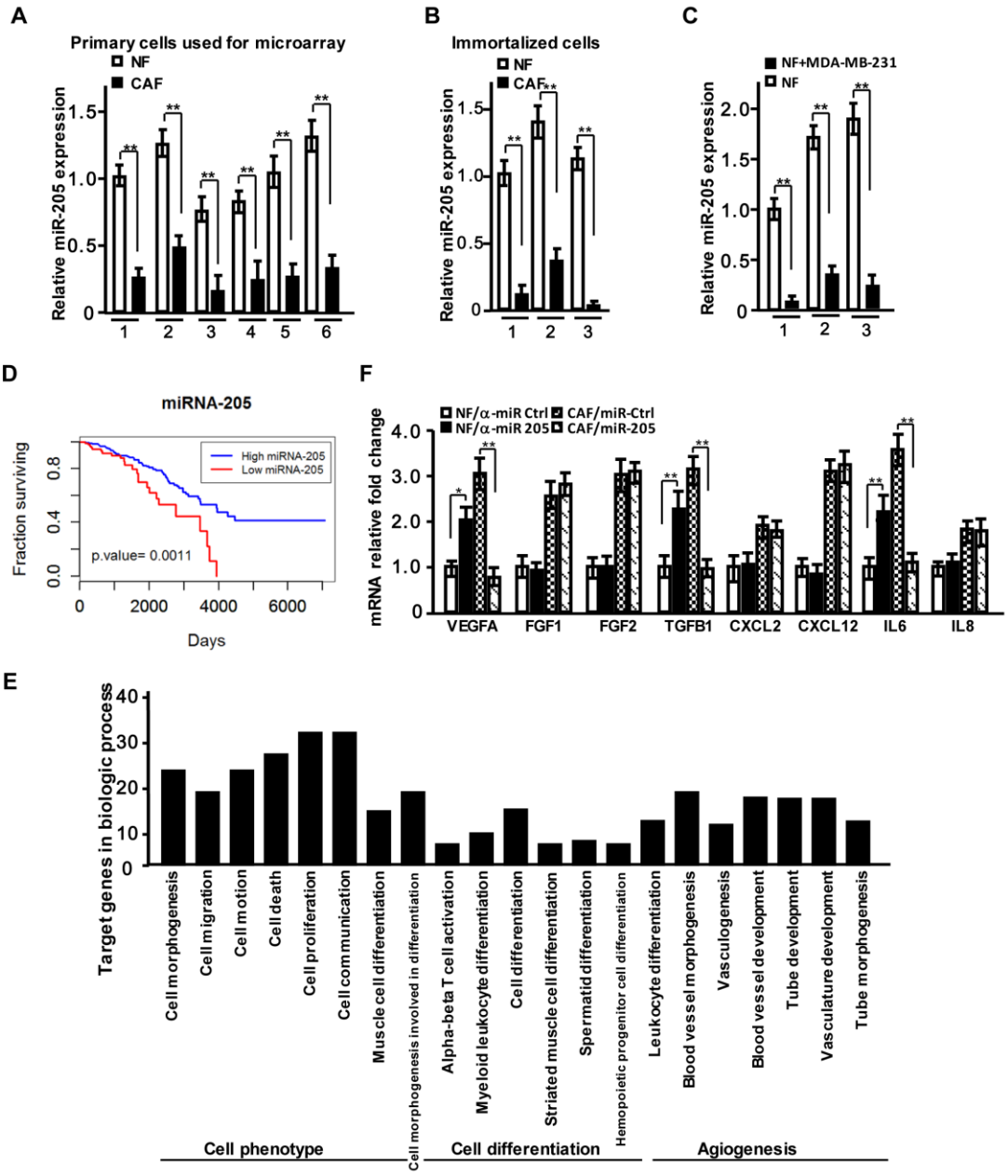

Figure S2. Downregulated miR-205 in CAFs is associated with angiogenesis.
(A-C) qRT-PCR to confirm the altered expression of miR-205 in the CAFs used for miRNA array-analysis (A), immortalized CAFs (B) and the educated fibroblasts by MDA-MB-231 cells (C). (D) The Kaplan-Meier survival analysis for patients with breast cancer with high- or low-expressed miR-205 using the database from The Cancer Genome Atlas (TCGA) (P=0.0011). (E) miR-205 target genes were predicted by PicTar and TargetScan and analyzed by DAVID v6.8. The target genes may involve in cell differentiation and angiogenesis. (F) qRT-PCR to determine expressions of miR-205 target genes, which are the known pro-angiogenic factors, in NFs stably transfected with miR-205 inhibitor or in CAFs with the ectopic miR-205. (n=3; *P<0.05, **P<0.01).

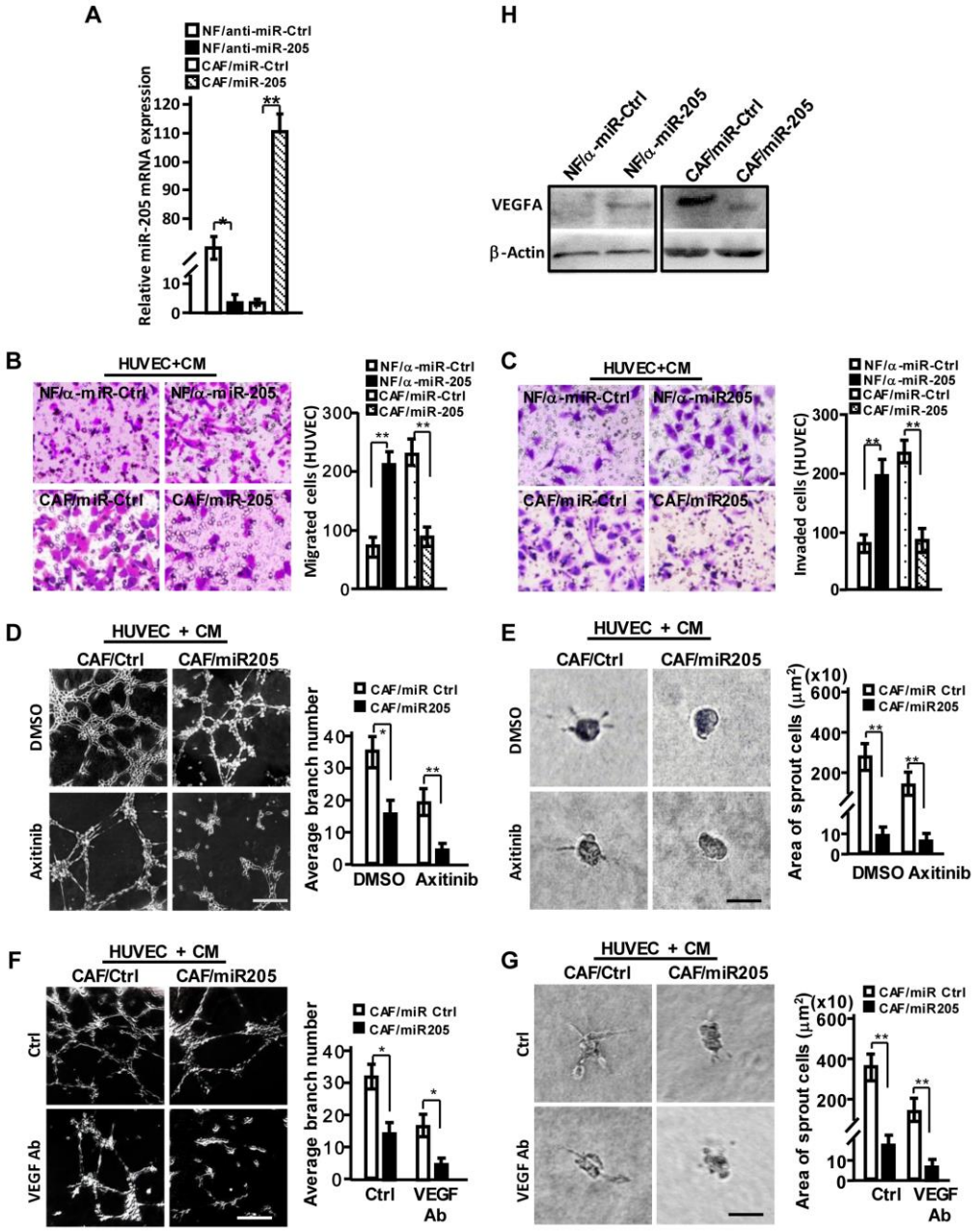

Figure S3. Downregulated miR-205 in stromal fibroblasts acts a pro-angiogenic role. (A) The expressions of miR-205 in NFs/anti-miR-205 and CAFs/miR-205 cells were measured by qRT-PCR. (B, C) HUVECs were cultured with CM from the indicated NFs or CAFs, cell migration (B) and invasion (C) potentials were tested by Transwell assay. (D-G) HUVECs were co-cultured on Matrigel in the presence of CM from CAFs/miR205 and its control cells with axitinib (D, E) or the neutralizing VEGF antibody (F, G), the representative images of tubule formation (D, F; Scale bar 300 μm) and sprouting (E, G; Scale bar, 150 μm) are shown. (H) Western blotting was used to detect VEGFA protein levels in NFs/anti-miR-205, CAFs/miR-205 and their control cells. β-Actin is the loading control. (n=3; *P<0.05; **P<0.01).

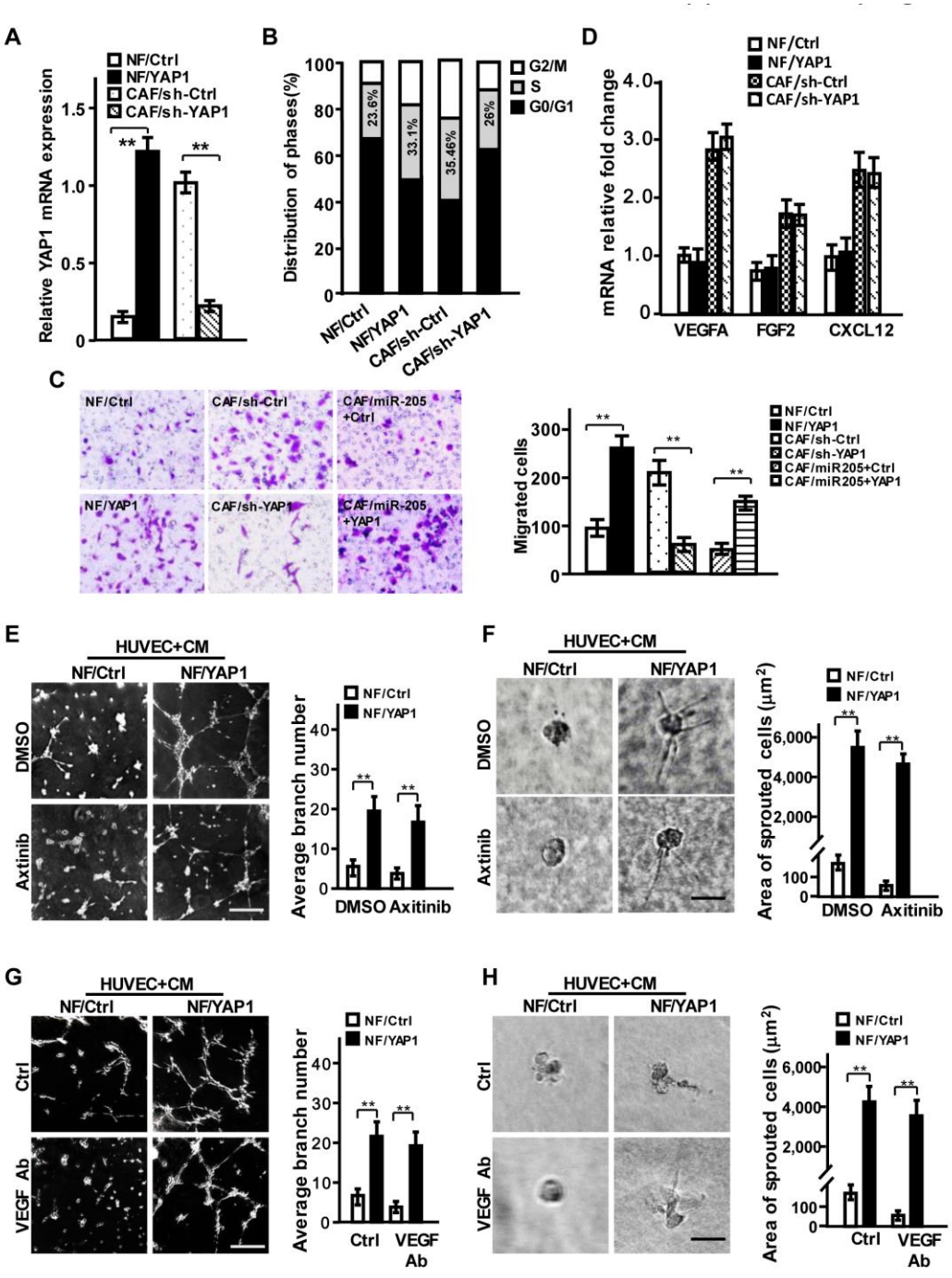

Figure S4. YAP1 activates NFs into CAFs and promotes invasion, tube formation and sprouting of HUVEC cells. (A) qRT-PCR analysis of YAP1 expressions in the NFs/YAP1 and CAFs/sh-YAP1 cells. (B) The S-phase cell ratio of NFs/YAP1, CAFs/sh-YAP1 and their controls was measured by flow cytometric assay. (C) Cell invasion was tested by Transwell assay for NF/YAP1, CAF/sh-YAP1, YAP1 knocked-down reprogramed NFs (NFs/anti-miR-205/sh-YAP1) and their control cells. (D) VEGF, FGF2 and SDF-1 expressions were detected by qRT-PCR in the indicated fibroblasts. (E-H) Representative images of tubule formation (E, G; Scale bar, 300 μm) and sprouting (F, H; Scale bar, 150 μm) of HUVECs after cultured in CM from NF/Ctrl or NF/YAP1 with VEGFR inhibitor axitinib or neutralizing VEGF antibody. (n=3; **P<0.01).

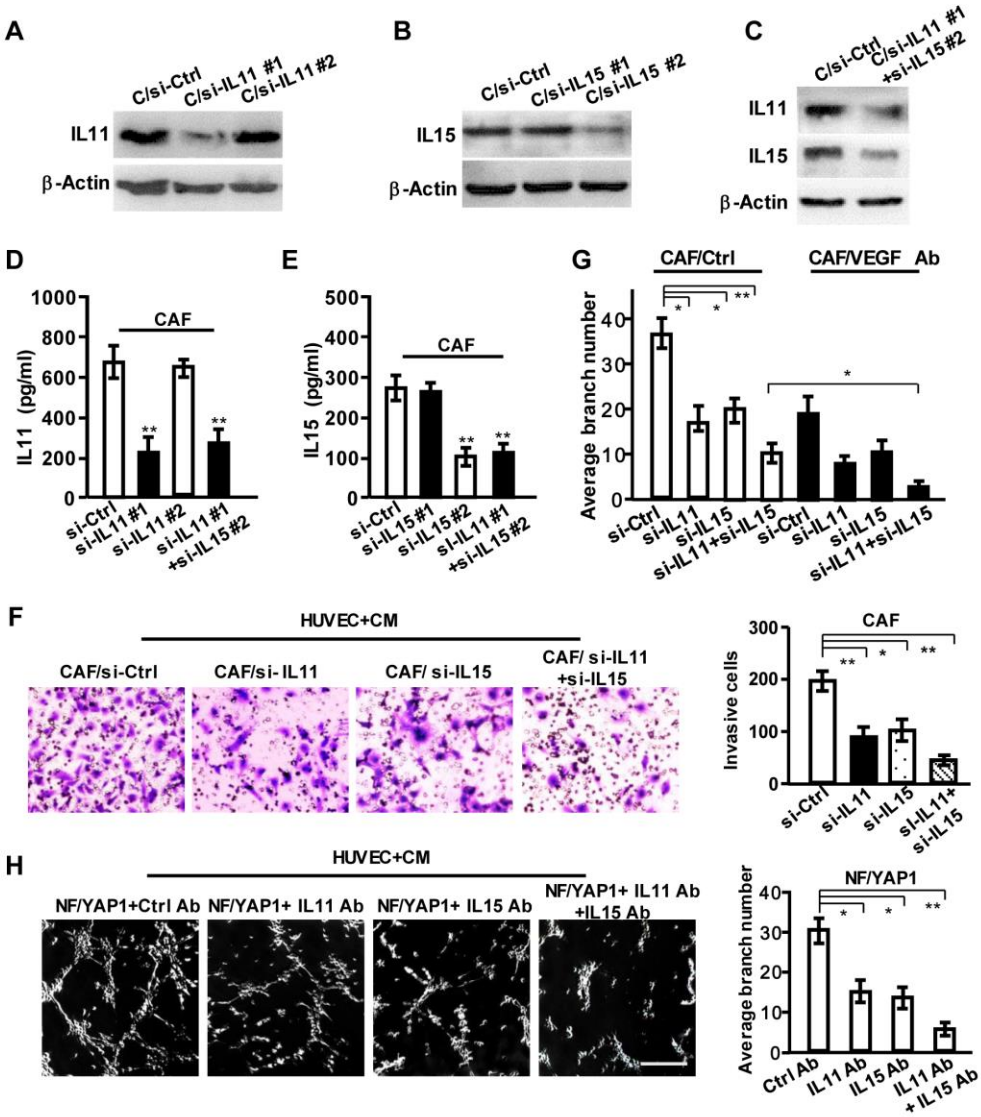

Figure S5. Knockdown of IL11 and IL15 in CAFs inhibits cell invasion and tubule formation of endothelial cells. CAFs were transfected with siRNAs against IL11, IL15 for 48 h, the indicated cells or their supernatants were collected and used in experiments. (A-C) Western blotting to analyze IL11 and IL15 expressions in CAFs with siRNAs against IL11 (A), IL15 (B) or IL11 and IL15 (C). β-Actin is a loading control. (D-E) ELISA analysis of IL11 (D) or IL15 (E) expression in the supernatant from the indicated CAFs. (F) The invasion ability of HUVECs toward CM from siRNA transfected-CAFs. (G) Tubule formation of HUVECs was measured under culture with CM from siRNA transfected-CAFs neutralized with VEGF antibody. (H) Tubule formation of HUVECs after cultured with CM from NF/YAP1 neutralized with IL11 and IL15 antibodies; Scale bar, 300 μm. (n=3; *P<0.05, **P<0.01).

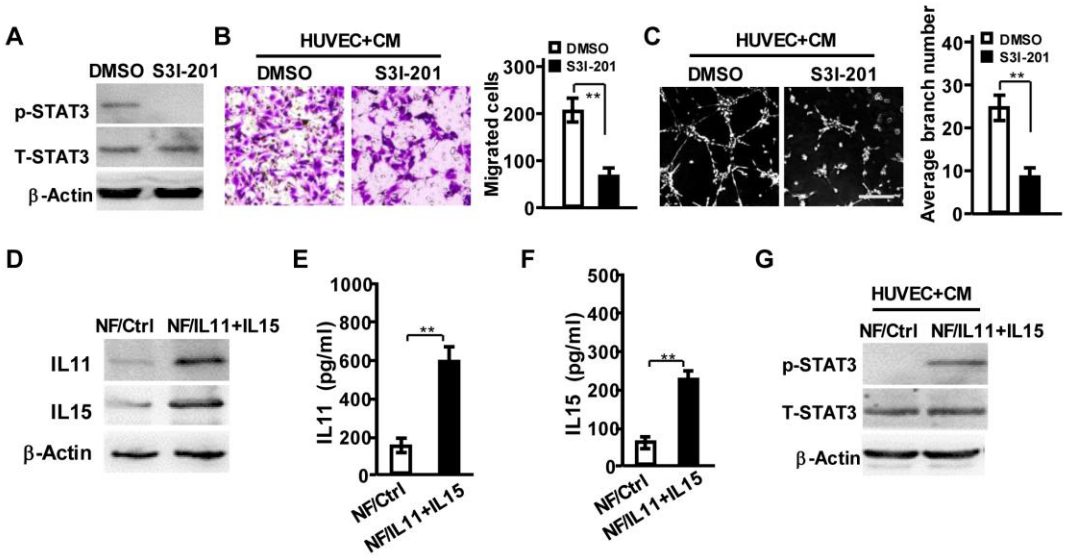

Figure S6. IL11 and IL15 derived from IL11- and IL15-overexpressing NFs directly activate angiogenic phenotypes of HUVEC cells. (A) Total and phosphorylated STAT3 proteins were verified by Western blotting analysis in HUVECs after being treated with S3I-201 for 6 hours. β-Actin is a loading control. (B) Transwell assay to examine cell invasion of HUVECs. HUVECs were seeded in the upper chambers with phosphorylated STAT3 inhibitor S3I-201, and CM from CAFs was added into the lower chambers. (C) The tubule formation ability of HUVECs was measured under treatment of CM from CAFs with or without S3I-201; Scale bar, 300 μm. (D-G) NFs were co-transfected with IL11 and IL15 vectors, the cells were collected for Western blotting and the supernatant for ELISA. (D) Western blotting analysis of IL11 and IL15 expressions in the indicated NFs. IL11 (E) and IL15 (F) in the supernatant of NF/Ctrl and NF/IL11+IL15 were measured by ELISA. (G) Western blotting to determine total and phosphorylated STAT3 proteins in HUVECs after being treated with CM from NF/Control and NF/IL11+IL15 cells. β-Actin is a loading control. (n=3; **P<0.01).

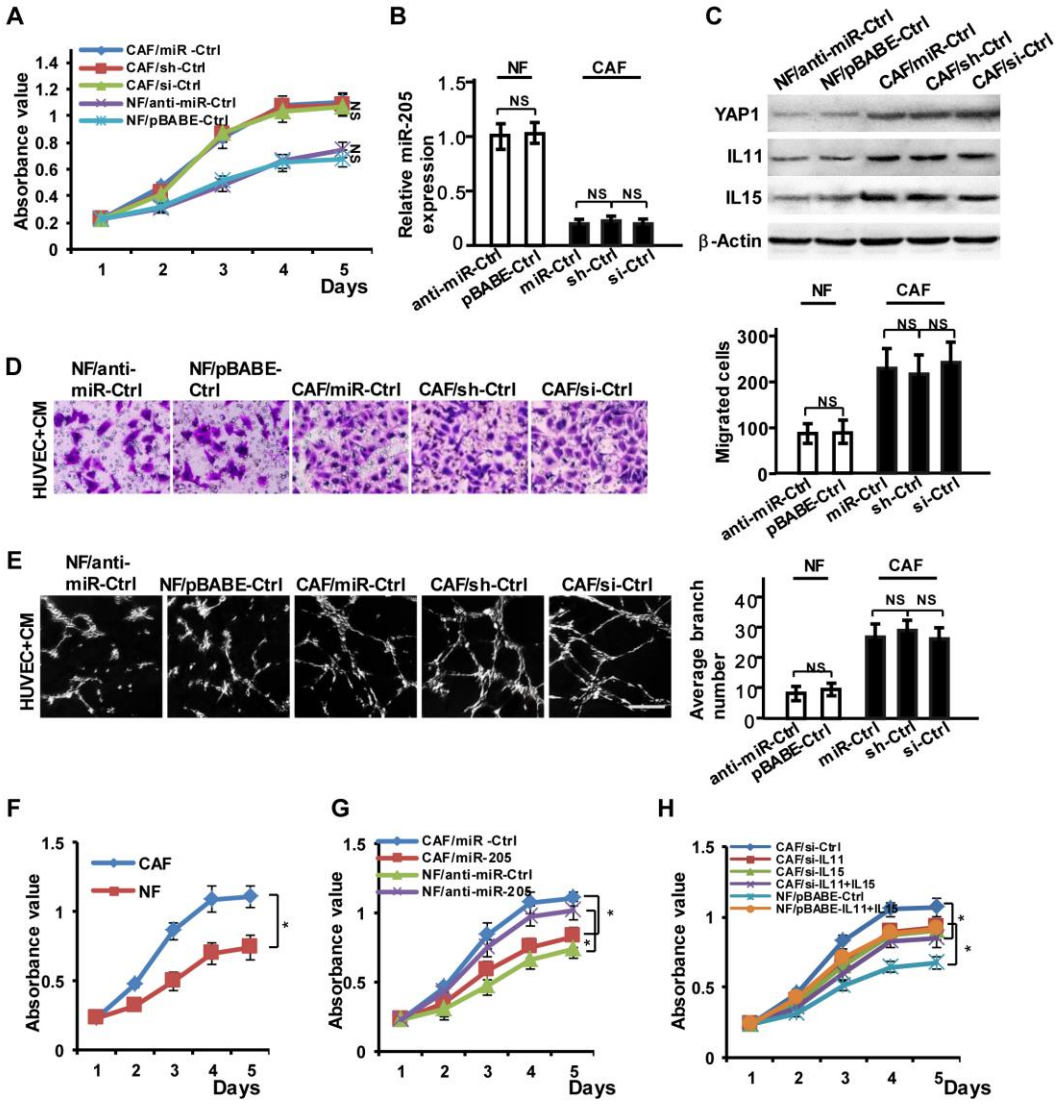

Figure S7. Biological characteristics of fibroblasts with different types of vectors. (A) Cell proliferation of the stromal fibroblasts transfected with different types of vectors was tested by MTT assay. (B) miR-205 expression in the stromal fibroblasts transfected with different types of vectors was tested by qRT-PCR. (C) Protein levels of YAP1, IL11 and IL15 in the stromal fibroblasts transfected with different types of vectors were determined by WB; β-Actin is the loading control. (D) Cell invasion of HUVECs toward CM from the stromal fibroblasts transfected with different types of vectors were tested by transwell assay. (E) The tubule formation ability of HUVECs was measured under treatment of CM from the stromal fibroblasts transfected with different types of vectors; Scale bar, 300 μm. (NS, not significant). (F-H) MTT assay was used to measure cell proliferation of NF and CAF (F), NFs/anti-miR-205, CAFs/miR-205 and their control cells (G), NFs/IL11+IL15, CAFs/si-IL11, CAFs/si-IL15, CAFs/si-IL11+IL15 and their control cells (H) in growth medium with 10%FBS. (n=3; NS, not significant; *P<0.05,)

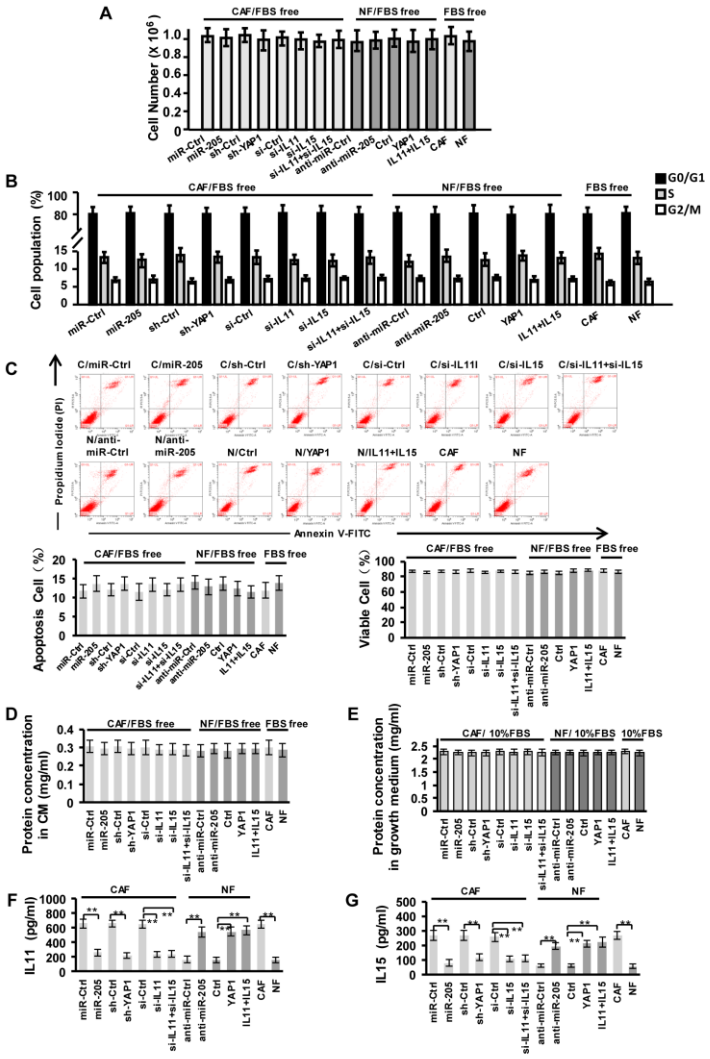

Figure S8. Validation of the conditioned medium (CM) derived from stromal fibroblasts. (A) Cell numbers of the indicated fibroblasts were counted when collection of conditioned medium (P>0.05). (B) Cell proliferation of the indicated fibroblasts were determined by S-phase cell ratio measured by flow cytometric assay when collection of conditioned medium (P>0.05). (C) Cell apoptosis was determined using Annexin V-FITC Kit and flow cytometric assay when collection of conditioned medium. The percentage of apoptosis cells include cells in early (Right lower quadrant) and late-stage apoptosis (Right superior quadrant), and percentage of viable cells (Left lower quadrant) were calculated (P>0.05). (D, E) The indicated stromal fibroblasts were cultured in FBS-free medium or growth medium with 10% FBS for 30 hours. Protein concentrations in supernatant derived from fibroblasts cultured in FBS-free medium (D) or cultured in growth medium (E) were tested by Bradford protein assay (P>0.05). (F, G) The protein concentrations of CM derived from activated fibroblasts were normalized by the protein concentration deviation value between activated fibroblasts and the control fibroblasts, and adjusted to the corresponding control cells; then L11 (F) and IL15 (G) in CM were measured using ELISA assay (n=3; **P<0.01).

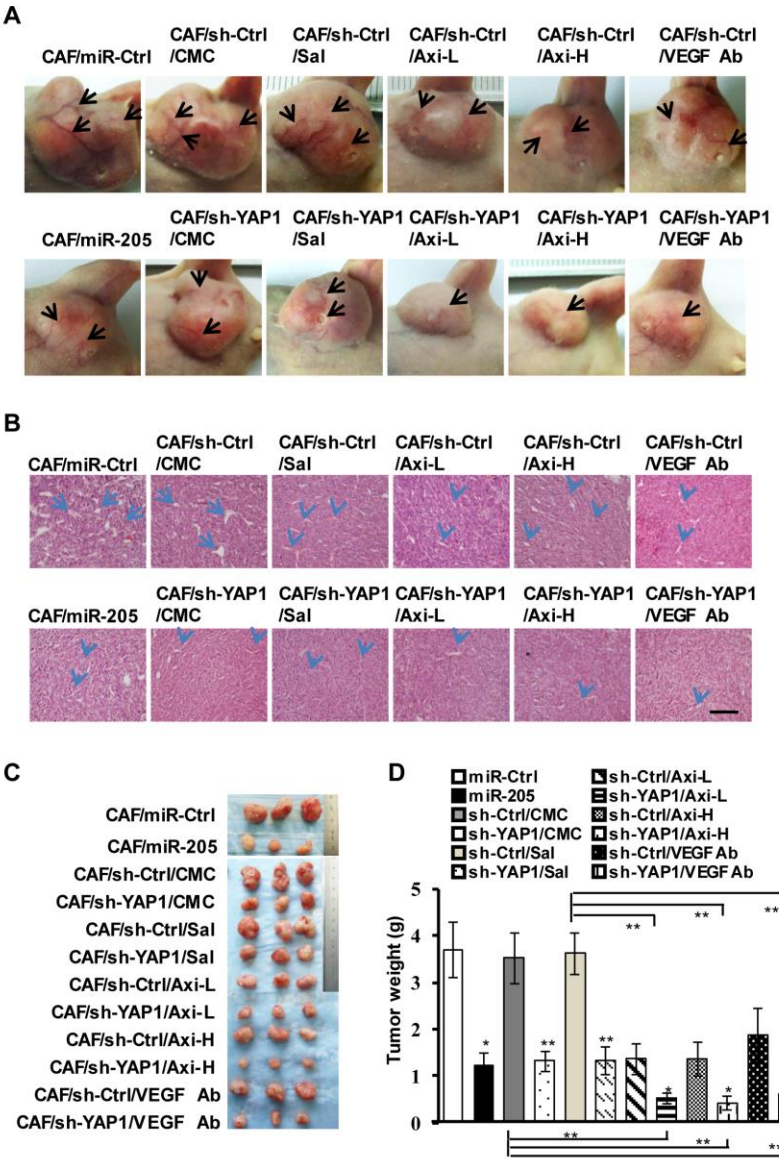

Figure S9. Tumor blood vessel and tumor weight measured in tumor-burden mice injected with CAF/miR-205, CAF/sh-YAP1 cells and their control cells. (A-D) The tumor-burden mice were treated with axitinib or the neutralizing anti-VEGF antibody as described in materials. Representative images of blood vessels on the tumor surface (A) and the blood vessel structures (labeled with blue arrow) in the H&E stained tumor tissues (B) are shown; Scale bar, 200 μm. (C) The representative tumor size in mice. (D) Tumor weight in the indicated mice. (n=5 per group; *P<0.05; **P<0.01).

Table S1 siRNA special against genes

Gene names	Sequences
Scramble	5’-TTCTCCGAACGTGTCACGT-3’
miR-205	5’-CAGACTCCGGTGGAATGAAGGA-3’
YAP1 #1	5’-GGTGATACTATCAACCAAA-3’
YAP1 #2	5’-CACATTAACGACTAGATTA-3’
IL11 #1	5’-GTGCCTTATTTATACTTAT-3’
IL11 #2	5’-ACACTTGACTGGGCCGTGA-3’
IL15 #1	5’-GGAGTTACAAGTTATTTCA-3’
IL15 #2	5’- CAGTCATTTTCTAACTGAA-3’

Table S2 **Primers for qRT-PCR**

Genes		Primer Sequences
U6	RT	AAAATATGGAACGCTTCACGAATTTG
miR-205	RT	GTCGTATCCAGTGCAGGGTCCGAGGTATTCGCACTGGATACGAC CAGACT
U6	F	CTCGCTTCGGCAGCACA
	R	AACGCTTCACGAATTTGCGT
Universal	R	GTGCAGGGTCCGAGGT
miR-205	F	GATCCTTCATTCCACCGG
YAP1	F	AGCTACAGTGTCCCTCGAAC
	R	CTTCCTGCAGACTTGGCATC
FXR1	F	AGTTACCGCCATTGAGCTA
	R	CCCCTTCAATTCTCACTCG
SLC4A4	F	ATTACTACCCCATCAACTCC
	R	CCTCCGTATTTTGAACACTCC
VEGFA	F	ATAAGTCCTGGAGCGTTCCCT
	R	TTAACTCAAGCTGCCTCGCC
FGF1	F	AGGGAATTACAAGAAGCCCAA
	R	GAGCCGTATAAAAGCCCGTC
FGF2	F	GCTGTACTGCAAAAACGGGG
	R	TAGCTTGATGTGAGGGTCGC
TGFB1	F	GGCGATACCTCAGCAACCG
	R	GTAGTGAACCCGTTGATGTCC
CXCL2	F	GAAAGCTTGTCTCAACCCCG
	R	GTTGGATTTGCCATTTTTCAGCA
SDF-1	F	TGCCCTTCAGATTGTAGCCC
	R	CTGTAAGGGTTCCTCAGGCG
IL6	F	AACAAATTCGGTACATCCTCGAC
	R	ATTTTCACCAGGCAAGTCTCC
IL8	F	TCCTGATTTCTGCAGCTCTGT
	R	CTCTGCACCCAGTTTTCCTTG
HMGB1	F	TGCTCTGAGTATCGCCCAA
	R	CATCAGGCTTTCCTTTAGCTC
CXCL14	F	TCATCACCACCAAGAGCGTG
	R	TTCCAGGCGTTGTACCACTT

Table S2 **Primers for qRT-PCR**

Genes		Primer Sequences
IL11	F	CCCTGAAGACCCTGGAGCCCGAG
	R	CACGGCCCAGTCAAGTGTCAGG
IL15	F	TTCCTAAAACAGAAGCCAAC
	R	CATGAATACTTGCATCTCCG
β-Actin	F	TGACGTGGACATCCGCAAAG
	R	CTGGAAGGTGGACAGCGAGG